Global Journal of Researches in Engineering: A
Mechanical and Mechanics Engineering
Volume 20 Issue 1 Version 1.0 Year 2020
Type: Double Blind Peer Reviewed International Research Journal
Publisher: Global Journals
Online ISSN: 2249-4596 & Print ISSN: 0975-5861

The Load Distribution with Modification and Misalignment and Thermal Elastohydrodynamic Lubrication Simulation of Helical Gears

By Jian-hua Xue, Zhen-hua Zhang & Huan-rui Wang

Abstract- A non-uniform model of the load per unit of length distribution of helical gear with modification and misalignment was proposed based on the meshing stiffness, transmission error, and load-balanced equation. The distribution of unit-line load, transmission error (TE), and contact press of any point on the contact plane were calculated by the numerical method. The feature coordinate system was put forward to implement the helical preliminary design and strength rating. The thermal elastohydrodynamic lubrication (EHL) model of helical gear was established, and the pressure, film, and temperature fields were obtained from the thermal EHL model. The maximum contact temperature and minimum film thickness solved by thermal EHL were applied to check the scuffing load capacity. The highest flash temperature and thinnest film occur in the dedendum of the pinion. The thermal EHL method to evaluate the scuffing load capacity is effective.

Keywords: helical gear; meshing stiffness; load distribution; scuffing load capacity.

GJRE-A Classification: FOR Code: 290501

Strictly as per the compliance and regulations of:

The Load Distribution with Modification and Misalignment and Thermal Elastohydrodynamic Lubrication Simulation of Helical Gears

Jian-hua Xue [α], Zhen-hua Zhang [σ] & Huan-rui Wang [ρ]

Abstract- A non-uniform model of the load per unit of length distribution of helical gear with modification and misalignment was proposed based on the meshing stiffness, transmission error, and load-balanced equation. The distribution of unit-line load, transmission error (TE), and contact press of any point on the contact plane were calculated by the numerical method. The feature coordinate system was put forward to implement the helical preliminary design and strength rating. The thermal elastohydrodynamic lubrication (EHL) model of helical gear was established, and the pressure, film, and temperature fields were obtained from the thermal EHL model. The maximum contact temperature and minimum film thickness solved by thermal EHL were applied to check the scuffing load capacity. The highest flash temperature and thinnest film occur in the dedendum of the pinion. The thermal EHL method to evaluate the scuffing load capacity is effective.

Keywords: helical gear; meshing stiffness; load distribution; scuffing load capacity.

I. Introduction

A helical gear is an common transmission device and has been widely used in all the fields, especially the machine under high speeds and heavy loads. The load distribution is the foundation of the gear preliminary design and strength rating process. It is known that the load distribution depends on the meshing stiffness of the tooth pair, and the load per unit of length is different at any point in the contact plane. The simple equations in standard ISO [1,2] to describe the load distribution, which is not in good agreement with experimental results. The contact lines of a helical gear are not parallel with the axial line, and the length of contact lines is dynamic changing in the meshing process.

Some studies on the meshing stiffness and load distribution of involute gears can be found in technical literature. Z. Chen et al. [3-6] studied the tooth mesh stiffness and transmission error via the finite element method (FEM). However, this method is feasible but has the problem no generality of the obtained results. Afterward, J.I.Pedreroet al. [7-9] proposed a method to calculated non-uniform load distribution along the line of contact from the minimum elastic criterion potential, which depends on the transverse contact ratio. Through this method, the author analyzed the bending strength and pitting load capacity of helical gears. But the balanced load equation was not considered in this method. Thus it can't provide the load distribution of any point on the contact plane, and it is hard to locate the maximum value of the load.

The heavy load and high-speed gear generate a lot of heat and temperature rise. High contact temperature of lubricant and tooth surfaces at the instantaneous contact position may lead to the break-down of the lubricant film at the contact interface. The scuffing failure is unpredictable and fatal for the gears system. Therefor the scuffing load capacity is of great importance in the process of helical gear system preliminary design and strength rating, especially for the heavy load and high-speed gear system. ISO [10,11] provides two methods, namely the flash temperature method and integral temperature method, to evaluate the scuffing load capacity of the gear system, nevertheless the load distribution use the simplified form and the flash temperature calculated based on the Blok flash temperature equation[12], which can't get the accurate flash temperature and need to attach a large safety factor to amend it.

The thermal elastohydrodynamic lubrication (EHL) is also a hot research topic. So far, most studies focused on the thermal EHL of spur gears. Wang and Cheng obtained a comprehensive research on a numerical simulation of the contact conditions of straight spur gear pairs[13,14]. L.M. Li proposed an inverse approach to establish the pressure, temperature rise, and apparent viscosity distribution in an EHL line contact[15]. Some methods and beneficial work to study on the EHL of spur gear, and a mass of cases were obtained, but these research mostly stay in the theoretical and ignore the practical application [16-19]. Besides the spur gears, the EHL research of helical gears is rare, no matter under the isothermal or thermal conditions. Recently, P.Yang and P.R.Yang used the multilevel multi-integration method to study the thermal elastohydrodynamic lubrication of tapered rollers in the opposite orientation; this model can be applied to the helical gear system [20]. These technical literature mentioned above mostly focus on the calculation method and directly offer the load; they can express the thermal EHL characteristic in theory but can't apply to

Author α σ ρ: Shaaxi Hande Axle Co., Ltd., Xi'an Shaanxi, China.
e-mail: xjh1986818@163.com

the actual conditions. The scuffing load capacity can be evaluated by the maximum contact temperature and minimum film thickness, which can be solved by the thermal EHL method. The literature of thermal EHL mostly focus on the temperature and film thickness of some single points [16-20]. The literature which makes the thermal EHL theory to design and check gear is absent.

This paper proposes a method to study the load per unit of length distribution of all the points on contact plane of helical gears accurately based on the balanced Load equation, transmission error, and meshing stiffness. The feature coordinate to simplify the preliminary design and strength check process of helical gears is established. Based on the load distribution, the thermal EHL model, which corresponds more to actual conditions, is put forward. The hydrodynamic pressure, film thickness, and contact temperature, as well as the flash temperature, to check the scuffing load capacity are calculated via the numerical method.

Nomenclature

b	gear face width, mm	η	viscosity of lubricant, Ns/ m^3
w	load per unit of length, N/m	r_{b2}	base radius of gear, m
m_n	normal module, mm	b_0	half width of the Hertzian line contact, m
ε_α	transverse contact ratio	P_H	maximum Hertzian pressure, Pa
ε_β	axial contact ratio	α	Braus viscosity-pressure coeffient, m^2/N
ε_γ	total contact ratio	β	Reynolds viscosity-temperature coefficient, k^{-1}
β	standard helix angle,(°)	x	contact coordinate in rolling direction ,m
β_b	base helix angle, (°)	z	coordinate across lubricant film, m
h	film thickness, m	$\lambda, \lambda_1, \lambda_2$	thermal conductivities of lubricant and solids, W/mk
E	elastic modulus, Pa	ρ, ρ_1, ρ_2	densities of lubricant and solids, $\mathrm{kg/m}^3$
t	temperature, K	c, c_1, c_2	specific heat of lubricant and solid, J/kgK
t_0	ambient temperature, K	P_{bt}	transverse circular pitch, m
r_{b2}	base radius of gear, m	P_{ba}	axial pitch, m
α_w	pressure angle (°)	n_1	rotational speed of pinion, $r\,\mathrm{min}^{-1}$
δ	deformation, m	k	stiffness of contact point, N/m
L	length of all the contact lines, m	TE	transmission error, μm

II. The Load Distribution Model of Helical Gear

a) The contact model of the helical gear under heavy load

For operating helical gear pair under heavy load, even though the driving pinion rotates at a constant speed, the gear as well as fall behind the angle $\Delta\theta$ than the theoretical location because of the deformation of driving and driven gear along the action line. As Fig.1 shows, the meshing condition viewing from helical gear transverse direction, the profile of the solid line is the theoretical location, and the dashed line is the actual location under deformation. N_1N_2 is the theoretical action line. Thus for any point K at the action line, the deformation along the action line is

$\delta_K = r_{b2} \cdot \Delta\theta$. Here assuming the stiffness of the contact point *TE* is k, then the load per unit of length of point *TE* is $w_K = k\delta_K$. For helical gears, the contact lines at the same time always more than one (depend on the total contact ratio), so setting L denotes the sum of the length of all the contact lines, the sum load of the helical gear is the integral of w_k, at any moment, it should be balanced to the extern load, the balanced load equation as follow:

$$\int_0^L w_K dl = \int_0^L k(l) r_{b2} \Delta\theta dl = \frac{9549P}{n_1 r_{b1}} = W_{sum} \qquad (1)$$

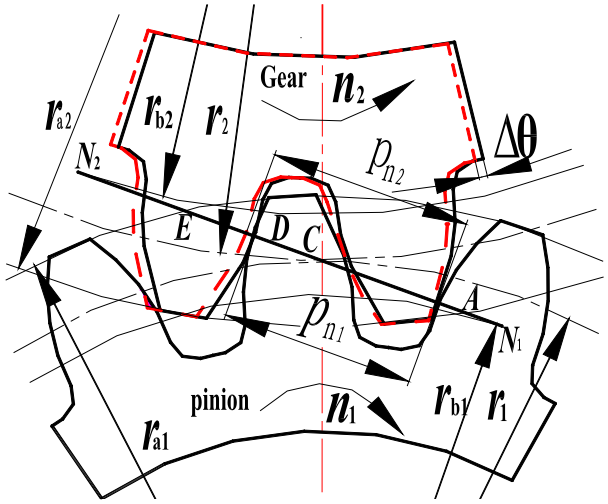

Fig. 1: The contact model of helical gear in transverse under heavy load

b) The sum length of the contact lines

The analysis model of the helical gear is shown as Fig.2, the contact plane $N_1N_2N_3N_4$ is the tangent plane of two gear base circle. K_1K_2 is one of the contact line. The actual action line is A_1E_1.The transverse contact ratio calculated by Equ.2.

$$\varepsilon_a = A_1E_1 / P_{bt} \qquad (2)$$

Where $P_{bt} = \pi \cdot m_t$ is the transverse circular pitch, m_t the transverse module.

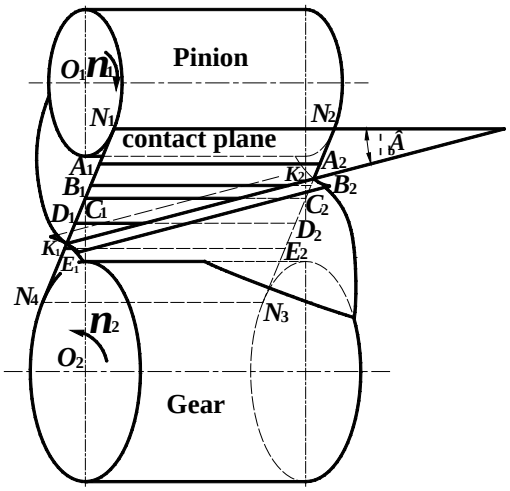

Fig. 2: The analysis model of the helical gear

Viewing from the transverse direction, for $\varepsilon_\alpha \subset (1,2)$, we can divide the A_1E_1 into three regions, A_1B_1, B_1D_1, and E_1D_1, the A1B1 and D1E1 are the double contact tooth regions (the number of tooth contact at the same time is 2), B_1D_1 is the single contact tooth region. So we can divide the actual contact plane into three regions. It shows as the Fig.3. The $A_1B_1A_2B_2$ and $D_1D_2E_1E_2$ are the double contact tooth regions, $B_1B_2D_1D_2$ is the single contact tooth region. In double contact tooth regions, the contact lines always occur double in the same location. The coordinate system is established to describe the actual contact plane $A_1A_2E_1E2$. The axial direction and action line direction are described by B and Γ [10]. Γ is the dimensionless parameter defined as follow:

$$\Gamma = (N_1K - N_1C) / N_1C$$

Where C is the pitch point, *K* the contact point, thus $\Gamma \in [\Gamma_{A_1}, \Gamma_{E_1}]$, $B \in [0, b]$.

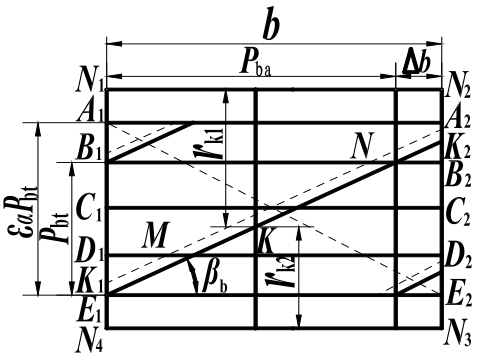

Fig. 3: Analysis model of helical real action plane

Now assuming $A_1$is the gear pair approach point (begin meshing), the contact line will move along with the line $A_1E_2$to the recess action point E_2. Axial contact ratio is expressed by the ε_β.

$$\varepsilon_\beta = b / P_{ba} = b \cdot \tan\beta_b / P_{bt} \tag{3}$$

The total contact ratio $\varepsilon_\gamma = \varepsilon_\alpha + \varepsilon_\beta$.When one of the ε_α and ε_β is an integer, the sum length of contact lines is constant. When $\varepsilon_\beta = n$, the sum length can be expressed as:

$$L_n = n\varepsilon_\alpha P_{bt} / \sin\beta_b \tag{4}$$

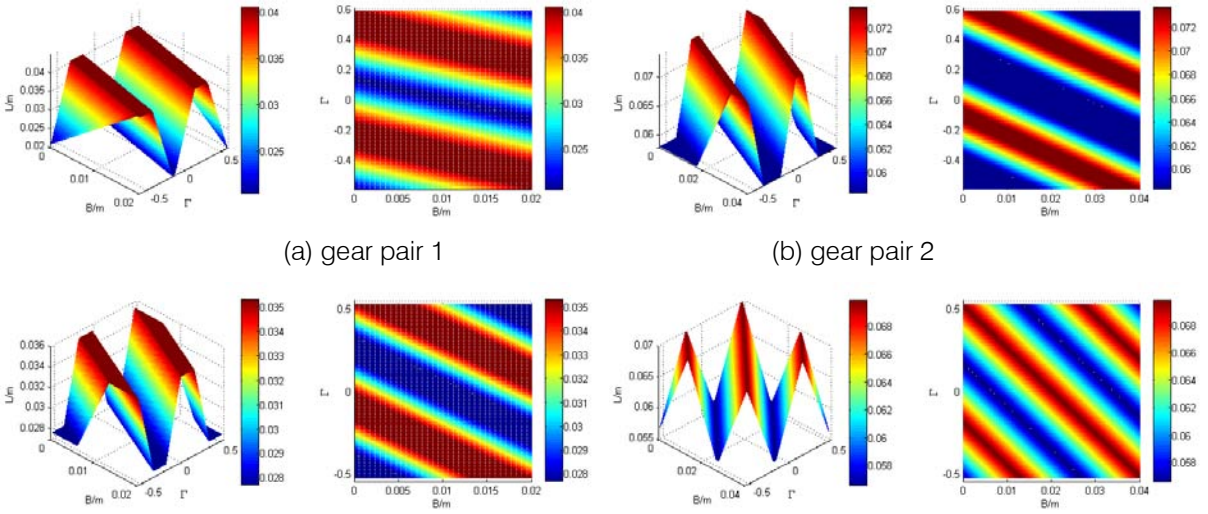

(a) gear pair 1 (b) gear pair 2

(c) gear pair 3 (d) gear pair 4

Fig. 5: The result of the sum length of contact lines

Table 1: Gear data and operating conditions

	Gear Pair 1	Gear Pair 2	Gear Pair 3	Gear Pair 4
Number of teeth (pinion/gear)	23/30	23/30	23/30	23/30
Normal pressure angle	20	20	20	20
Normal module, mm	3	3	3	3
Face width, mm	20	40	20	40
Input power(kw)	50	50	50	50
Modulus of elasticity E_1/E_2, GPa	206/206	206/206	206/206	206/206
Poisson ratio, ν_1/ν_2	0.3/0.3	0.3/0.3	0.3/0.3	0.3/0.3
Helix angle,°	9.8	9.8	20.2	20.2

Pinion speed, $r/\min^{-1}$	2000	2000	2000	2000
transverse contact ratio ε_α	1.59	1.59	1.49	1.49
Axial contact ratio ε_β	0.36	0.72	0.73	1.47
total contact ratio ε_γ	1.95	2.31	2.22	2.96

The length distribution of contact lines with the parameters listed in Table 1 shows as Fig.5. For different gear pairs, the distribution of load per unit of length is different. Compare the gear pair one and two or three and four, the face width doubled, and the length of the contact line almost double as well. The wider the tooth width, the longer the total length. But the value that the maximum minus the minimum has the upper limit value. We are letting the length ratio $\varsigma = L_{\min} / L_{\max}$, the length ratio under different helix angle is show in Fig.6. It is obvious that when $\varepsilon_\gamma < 2$, the length ratio is only 0.5, and the fluctuation of length is greatly, the maximum is as double as the minimum length. When $\varepsilon_\gamma > 2$, the length ratio is close to 1.

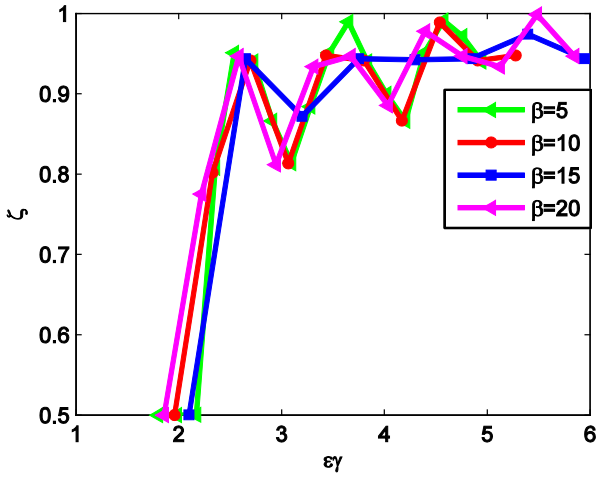

Fig. 6: The length ratio varying with the total contact ratio

c) The tooth meshing stiffness

The gear profile is a complex graphics and can be simply as the combination of a rectangle and a trapezium, as the Fig.7 shows. The gear deformation includes the bending deformation, shear deformation, and contact deformation. The total is the sum of the rectangle deformation and trapezium deformation. The total of the contact deformation point along the action line can be expressed as the sum of the bending deformation δ_B, shear deformation, δ_S and lean deformation δ_G.

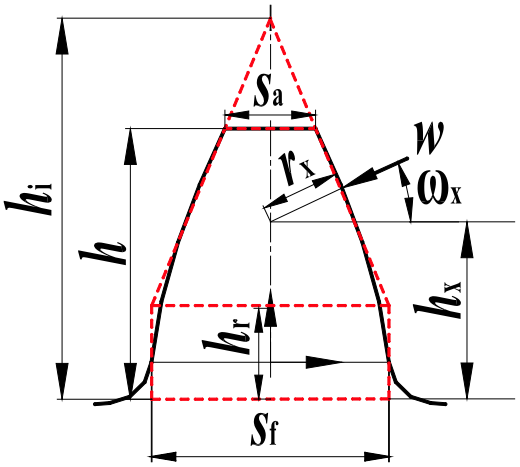

Fig. 7: The stiffness analysis model of gear tooth

$$\delta = \delta_{Br} + \delta_{Bt} + \delta_S + \delta_G \quad (5)$$

Where δ_{Br} and δ_{Bt} means the bending deformation of rectangle and trapezium, δ_S notes the shear deformation.

$$\delta_{Br} = \frac{12w\cos^2\omega_x}{E_i S_f^3}\left[h_x h_r (h_x - h_r) + \frac{h_r^3}{3}\right]$$

$$\delta_{Bt} = \frac{6w\cos^2\omega_x}{E_1 S_f^3}\left[\frac{h_i - h_x}{h_i - h_r}\left(4 - \frac{h_i - h_x}{h_i - h_r}\right) - 2\ln\frac{h_i - h_x}{h_i - h_r} - 3\right](h_i - h_r)^3$$

$$\delta_S = \frac{2(1+\nu_1)w\cos^2\omega_x}{E_i S_f}\left[h_r + (h_i - h_r)\ln\frac{h_i - h_r}{h_i - h_x}\right]$$

$$\delta_G = \frac{24wh_x\cos^2\omega_x}{\pi E_i S_f^2}$$

Where h is the height of the tooth, h_x the height of contact point, h_r the height of the rectangle, ω_x the pressure angle of the contact point, $h_i = \frac{hS_f - h_r S_a}{S_f - S_a}$, ν_i notes the Poisson's ratio of pinion, E_i the elastic modulus of pinion or gear, w the load per unit of length.

When a pair of tooth meshing, the sum deformation along the action line can be described as the Equ.6。

$$\delta_\Sigma = \delta_1 + \delta_2 + \delta_{PV} \quad (6)$$

Where $\delta_{PV} = \frac{2w[(1-\nu_1^2)+(1-\nu_2^2)]}{\pi E}$ is the contact deformation of the meshing point, so the stiffness of this point can be expressed as Equ.7.

$$k = w/\delta_\Sigma \quad (7)$$

Fig.8 shows the distribution of stiffness along the action line; the maximum occurs close to the pitch point. The regulation of stiffness is similar to the inverse unitary potential $v(\xi)$ in Ref. [7-9], which all reflect the capacity that the tooth bears the deformation.

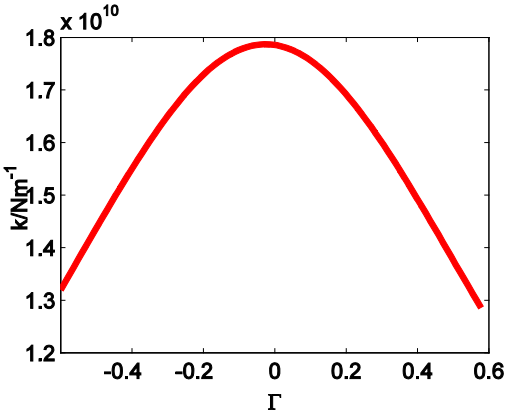

Fig. 8: Gear teeth stiffness along the action line of gear pair 1

d) The load distribution calculation process of helical gear

In Fig.3, the sum length is shown as follow:

$$W_{sum} = \int_0^{L_{sum}} k(l)\cdot TE\cdot dl \quad (8)$$

For the convenience of numerical calculation, the line A_1E_1 is divided into N nodes, and $l_\Delta = A_1E_1/(N-1)$, so the total load can be expressed as Equ.9, the number of the contact line is m.

$$W_{sum} = \sum_{j=1}^{m}\sum_{i=1}^{n} k_{ij}\max((TE_{ij} - \Delta_x), 0)\cdot l_\Delta / \sin\beta_b \quad (9)$$

The load distribution calculation process of helical gear is shown as Fig.9. According to the equations above, we can calculate the load distribution of every point on the contact plane. Firstly, letting $L=L_0$, $k=k_c$, and TE_0 will be calculated; secondly, from the Equ.9, the sum load was obtained, then modified the *TE* according to Equ.10, until the sum load satisfied the Equ.11, then repeat this process until the results of all points were obtained.

$$TE_1 = \frac{w_{sum}}{w}TE_0 \quad (10)$$

$$\frac{|w - w_{sum}|}{w_{sum}} \le 10^{-5} \quad (11)$$

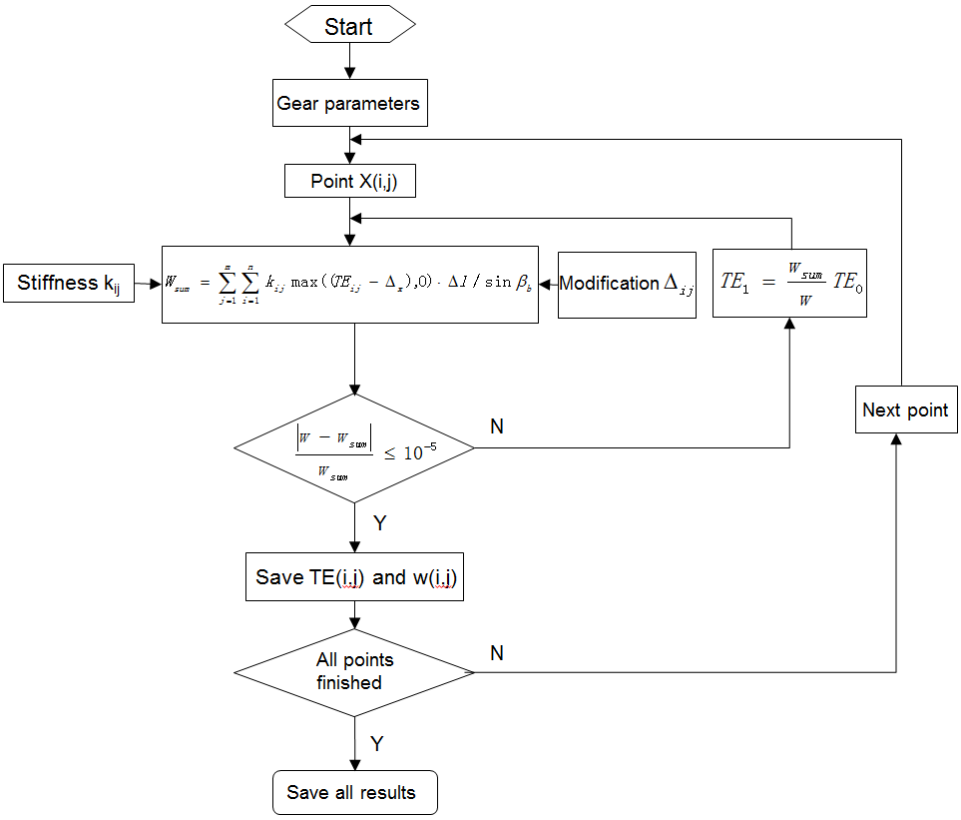

Fig. 9: The load distribution calculation process of helical gear

e) *The contact stress of the helical gears*

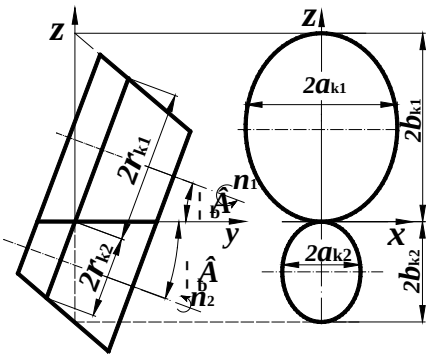

Fig. 10: The contact model of helical temperature

The contact model of the helical gear can be regarded as two tapered rollers [20]. In this model, the actual geometric model is two oval in oxz coordinate systems, and the geometric parameters as follows:

$$a_{Ki}\big|_{i=1,2} = \frac{r_{Ki}\cos^2\beta_b}{1-2\sin^2\beta_b} \quad b_{Ki}\big|_{i=1,2} = \frac{r_{Ki}\cos\beta_b}{1-2\sin^2\beta_b} \tag{12}$$

Where the subscript 1 means the pinion, 2 for gear. The curvature of the contact point of two oval are as follows:

$$R_i\big|_{i=1,2} = \frac{a_{Ki}^2}{b_{Ki}} = \frac{r_{Ki}\cos^3\beta_b}{1-2\sin^2\beta_b} \tag{13}$$

According to the Hertz contact theory, the maximum contact press of the helical gear is expressed as Equ.14.

$$\delta_H = \frac{\pi}{4}\sqrt{\frac{Ew}{2\pi R}} \tag{14}$$

Where $R = \frac{R_1 R_2}{R_1 + R_2}$ the curvature sum, E is equivalent to Young's modulus, $\frac{1}{E} = \frac{1}{2}\left(\frac{1-\nu_1^2}{E_1} + \frac{1-\nu_2^2}{E_2}\right)$.

f) The load distribution calculation of helical gear without modification

In the calculation process, the modification, setting Δ_{ij} to 0, then the transmission and the unit-line load of contact plane can be obtained. The three-dimension unit-line load distribution is shown in Fig.11. The load distribution on the contact plane is not only depends on the transmission error, but also depends on the stiffness distribution. The value of the load is small in the dedendum and addendum region of helical gear, and large close to pitch point. For the different helix angles and different face width, the load distribution is different. As we know, the sliding speed is maximum in the dedendum or addendum. From the 4 cases, the biggest occurs in the begin meshing and engaging-out point of, the helical contact plane.

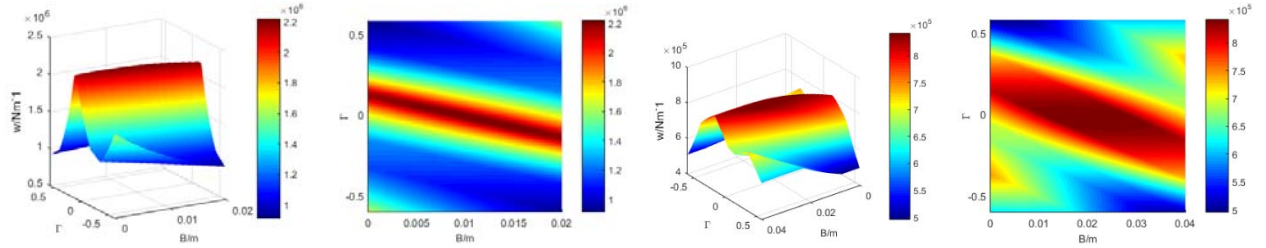

(a) Gear pair 1 (c) Gear pair

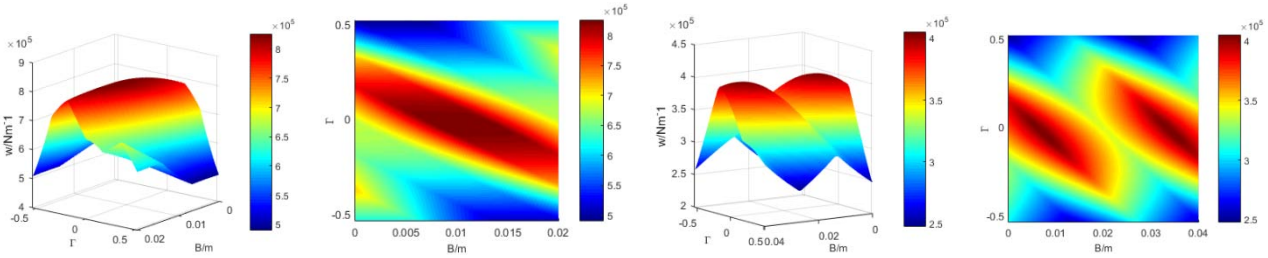

(a) Gear pair 3 (c) Gear pair 4

Fig. 11: Unit-line load distribution of helical gears

The load distribution solved in this paper is in good agreement with the results which occur in Ref.8 by the finite elements method (FEM). The results show that the contact stress solved by FEM is larger near the pitch point and small in the dedendum and addendum region. Thus the load distribution in this paper is consistent with the actual condition to a great extent without the consideration of the end effect, the machine error, and assembly error.

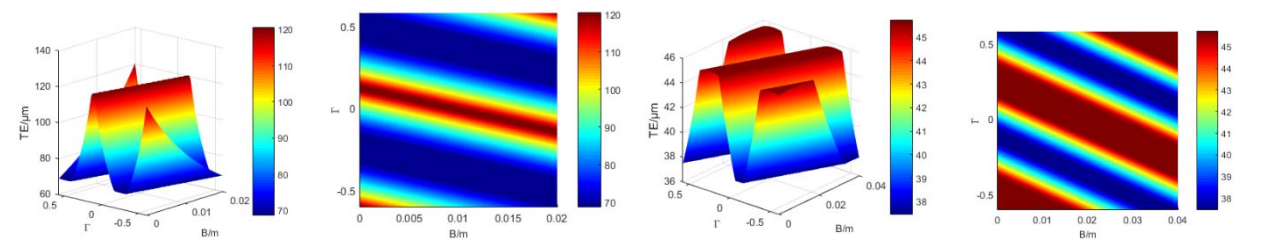

(a) Gear pair 1 (b) Gear pair 2

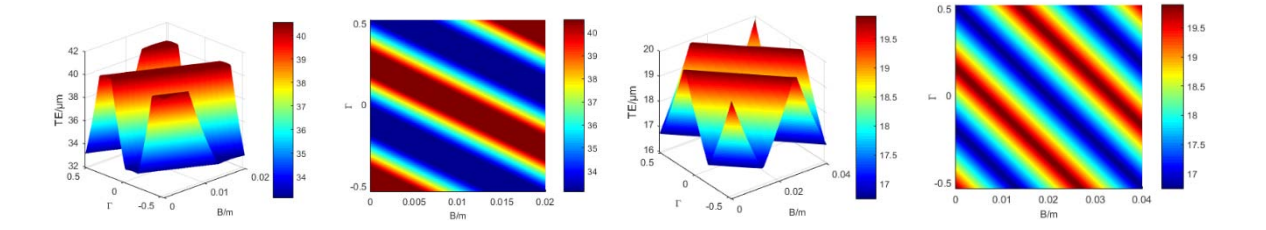

(c) Gear pair 3 (d) Gear pair 4

Fig. 12: The transmission error of the helical gears

The transmission errors of helical gear pairs shown in Fig.12, its distribution law corresponding to the distribution of length. The fluctuation of transmission error is the main indicator of the vibration and dynamic load. It is significant to choose the advisable helix angle and face width to make the fluctuation of transmission error minimum.

The contact press distribution of the helical gears is shown in Fig.13. It is similar to the unit-line load. But the contact stress of foot is greater than that of top of pinion. It is because the sum radius of the curvature of the root is smaller than that of the tooth top. For a helical cylindrical gear without modification, the maximum contact press is located at the engagement of the pinion root. As shown in Fig.14, it is a fatigue pinion of an electric axle after the loading bench test, fatigue pitting at the meshing point of the root of the pinion.

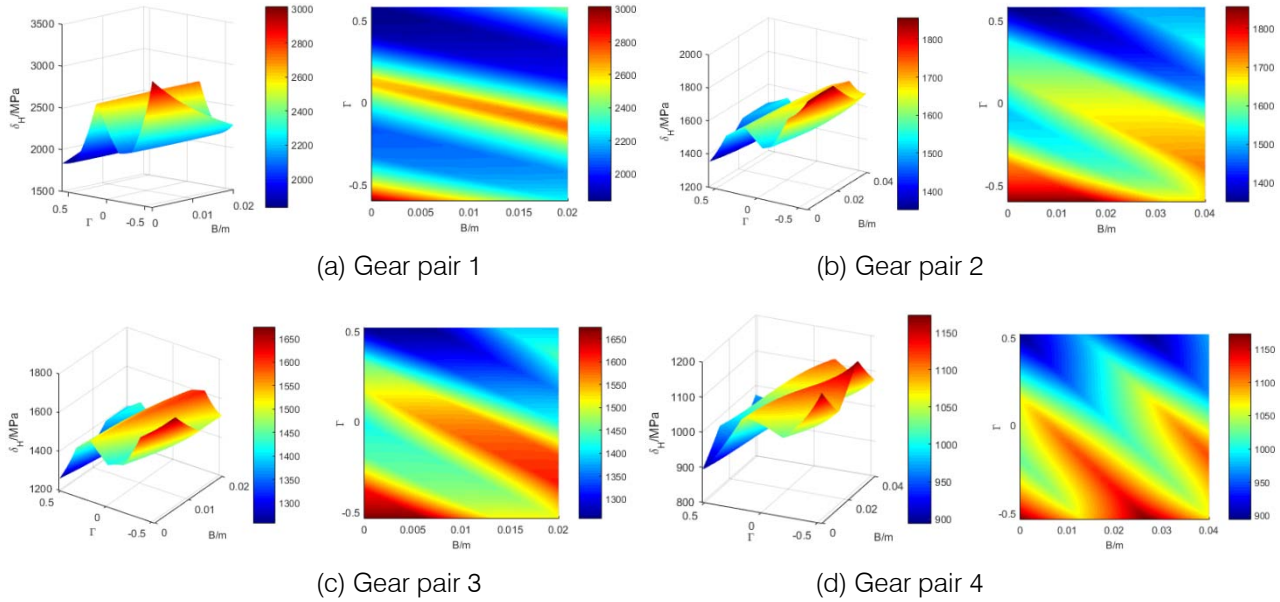

(a) Gear pair 1 (b) Gear pair 2

(c) Gear pair 3 (d) Gear pair 4

Fig. 13: The contact press of the helical gears

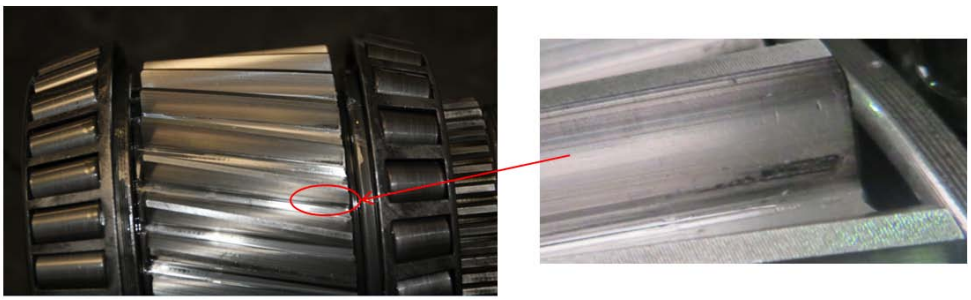

Fig. 14: The fatigue pitting at the meshing point of helical gear

g) The contact stress with the modification and misalignment

In practical application, the tooth surface of helical gear needs to be modified. For one reason, the maximum contact press located at the engagement of the pinion root. For the second reason, the shafts, bearings, and the housing will be deformed under the heavy load.

The modification includes the profile modification and helix modification. Profile modification includes profile crowning, pressure angle modification, tip relief, and root relief. The helix modification includes lead crowning, helix angel modification, and end relief. According to the calculation method in Fig.9, the transmission error(TE), unit-line load distribution, and contact press distribution of helical gear could be obtained. For the four gear pairs in table 1, the modification parameters are shown as table 2.

Table 2: Modification parameters

Modification form	Modification/um
profile crowning(barreling) C_α	10
Lead crowning C_β	10
tip relief	5
End relief	0
Helix angle modification fHβ	0
Pressure angle modification, fHα	0

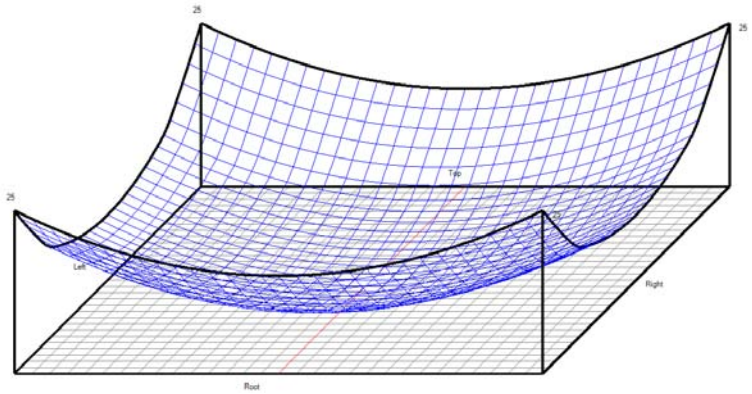

Fig. 15: Modification distribution of contact plane

The modification distribution of the helical gear contact plane is as shown in Fig.15. And the contact press of helical gear is shown in Fig.16. After modification, the contact press distribution of the tooth surface has been greatly improved. The maximum pressure transferred from the meshing point of the pinion root to the central area of the contact surface.

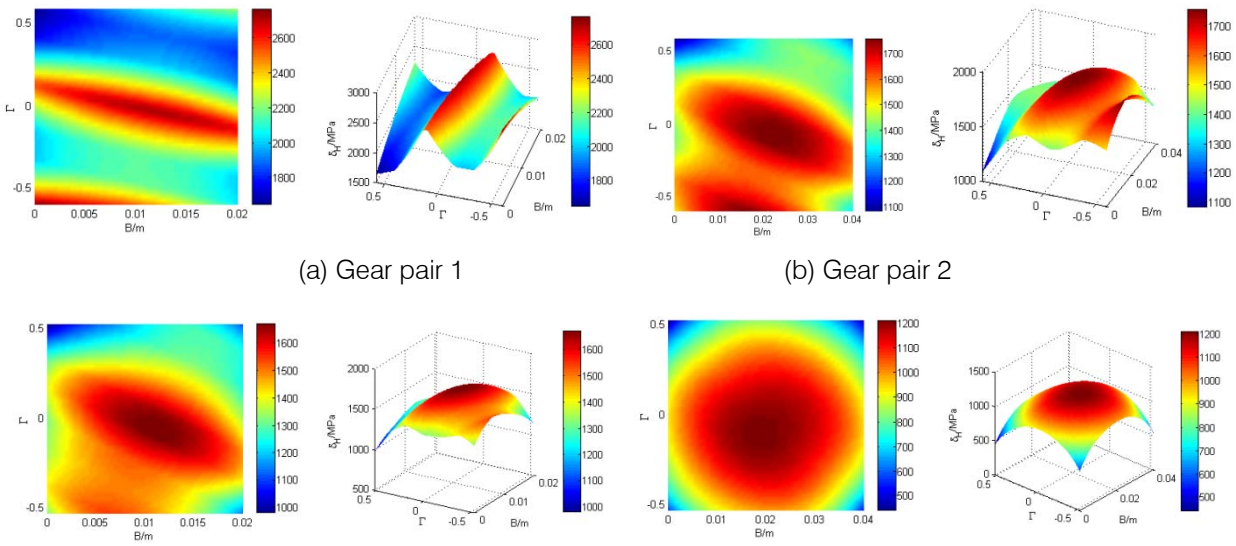

(a) Gear pair 1 (b) Gear pair 2

(c) Gear pair 3 (d) Gear pair 4

Fig. 16: The contact press of the helical gears with modification

In a transmission system, due to the deformation of the transmission shaft, the machining error of the gearbox, and the changes of the bearing stiffness, the gears pair will operate with misalignment. The contact state with misalignment can be simulated by the helix angle modification. Take gear pair 4 for example, the contact press distribution with different helix modification is shown in Fig.17. With the increase of tooth inclination deviation, the contact stress inclines to one end, and the maximum stress is also increasing.

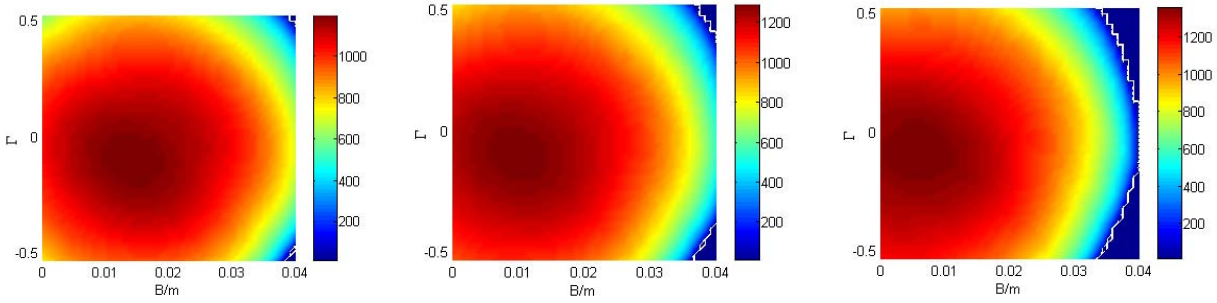

(a) fHβ=10um (b) fHβ=20um (c) fHβ=30um

Fig. 17: The contact press distribution with helix modification

h) The feature coordinate system

From the above analysis, all the results in the contact plane were calculated by the numerical method. But in the preliminary design and strength rating process of helical gear, our focus is the maximum stress or the highest contact temperature of the contact plane. For the helical gear, the sliding speed is large in the addendum and dedendum region, and most scuffing failure occurs in these regions. The sliding speed approximately zero in the region close to the pitch point, so it is safer than the addendum and dedendum region. The 3-dimensional load distribution covers all the information about the contact plane, but it is time-wasting and not intuitionistic. So the feature coordinate system should be established.

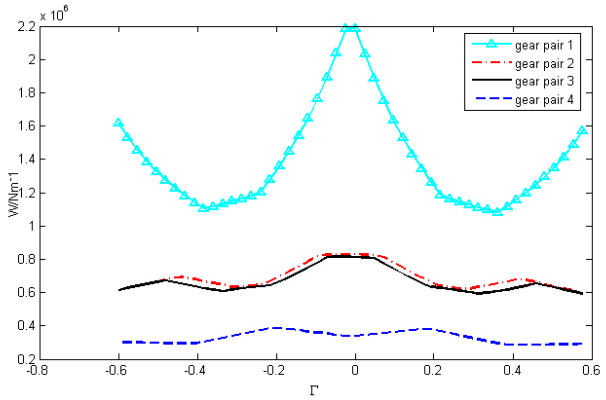

Fig. 18: Unit-linear load and transmission error distribution

In Fig. 3, the line A_1E_2 is recommended as the feature coordinate system, marked by Ψ, defined the same as Γ. The A_1 is the approach point (begin meshing), and E_2 is the recess point. The parameters in feature coordinate cover both the tooth profile and axial information. The unit-line load distribution along with the feature coordinate is shown in Fig.18.Compared the feature coordinate and 3-dimension coordinate, the maximum is the same in the addendum and dedendum region, the value in the feature coordinate system is a little lower than the three-dimension coordinate close to the pitch point, because the dangerous region of helical gear is the addendum and dedendum, so that the feature coordinate can satisfy the need of design and strength ratting. Furthermore, the feature coordinate is more succinct than the three-dimension. From the load distribution of gear pair 1 and 3, or gear pair 2 and 4, the helix angle has influenced a lot on the load distribution, in the case, the helix angle from the 9.8 to 20.2, and the maximum load per unit of length from the 3.8×10^5 N/m to 2.7×10^5 ,so it is important to choose appropriate helix angle, tooth height, and face width to optimize the load distribution and minimize the dynamic load.

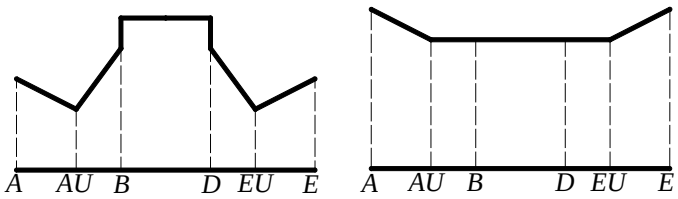

(a)Narrow helical gear (b) Wide helical gear

Fig. 19: Load sharing factor for the narrow helical gear and wide helical gear of ISO

In the Ref.10, the load distribution of narrow helical gear is given as the Fig.19, the buttressing effect near the end points A and E of the line of action, compared the results in this paper, the load distribution is similar with the gear pair 1,but is different from the gear pair 2, so the ISO can reflect the characteristic to some extent. Still it can't adapt to all the conditions. In this way, the method proposed by this paper is effective, and the point AU and EU is given by Equ. 15.

$$\Gamma_{AU} - \Gamma_A = \Gamma_E - \Gamma_{EU} = 0.2\sin\beta_b \tag{15}$$

In the ISO standard theory, the helical gear with the total contact ratio $\varepsilon_\gamma < 2$ was treated similarly to spur gears as well as the buttressing effect. And the wide helical gear ($\varepsilon_\gamma > 2$) was assumed to act near the ends A and E along with the helix teeth over a constant length. From the Fig.6, we know that even though the $\varepsilon_\gamma > 2$, the fluctuation is considerable for some parameters. So the ISO standards are stereotypical and inaccurate.

III. The Thermal Elastohydrodynamic Lubrication of Helical Gears

a) The analysis model of the thermal elastohydrodynamic lubrication

When gears pair subjected to heavy loads, the lubricating film may not separate the surfaces adequately, leading to localized damage of the tooth surface. This type of failure is known as scuffing and it is checked by maximum contact temperature and film thickness. Scuffing failure may occur at any stage during the lifetime of a set of gears, and it may lead to failure in a few of hours if the contact temperature is too high. So it is significant to research the scuffing load capacity of the gears.

The high contact temperature is the main reason for scuffing failure, and the interfacial contact temperature conceived as the sum of two components, namely the bulk and flash temperature [10]. The bulk temperature fields are constant with time. Nevertheless, the flash temperature varies with time, and only appears in the interface of pinion and gear. In the thermal steady state, the bulk temperature of the tooth is higher than the ambient oil temperature.

$$t_B = t_M + t_f \tag{16}$$

Where t_B is the contact temperature, t_M the bulk temperature, and t_f the flash temperature. The bulk temperature can be calculated by the finite element method (FEM). For the pinion of the pair 1, the bulk temperature is 360K (87℃), the ambient oil temperature is 60℃.

The internal energy of oil film will increase due to the compression and viscous damping, and the temperature of oil film and tooth will rise because of the heat convection and conduction. After some time, the whole system will be on a thermal steady state. The bulk temperature of gear was higher than the ambient oil temperature. Therefore, in the inlet zone, the tooth profile is the heat source to heat the lubrication film, and the lubrication film temperature will rise instantly as high as the bulk temperature because that the lubricating film thickness is so thin. Then the temperature of the lubrication film will get higher due to the compression and viscous damping. In this region, the lubricating film is the heat source to heat the gear by convection and conduction. The ambient temperature was chosen as the inlet temperature in the technical literature [16-20]. By this means, the interface temperatures of the inlet contact region solved by the numerical method will lower than the interface bulk temperature; It is not in good agreement with the fact. In this paper, the interface bulk temperature was taken as the inlet temperature, which is more reasonable.

b) The thermal elastohydrodynamic lubrication equations

i. *Reynolds equation*

For the thermal steady state, the Reynolds equation of helical gear can be expressed in the following form as:

$$\frac{\partial}{\partial x}\left(F_2\frac{\partial p}{\partial x}\right) = u_2\frac{\partial(\rho h)}{\partial x} - (u_2 - u_1)\frac{\partial}{\partial x}\left(\frac{\rho F_1}{F_0}\right) \tag{17}$$

Where $F_0 = \int_0^h 1/\eta dz$, $F_1 = \int_0^h z/\eta dz$, $F_2 = \int_0^h \rho \cdot z/\eta(z - F_1/F_0)dz$.

The sliding speed of contact point:

$$u_i\big|_{i=1,2} = \pi \cdot n_i R_i / 30 \quad (18)$$

In this equation, the mass density and the viscosity of lubricant can be described by Dowson and Higginson temperature-pressure–density relationship [21] and Roelands temperature-pressure–viscosity relationship [22] can be expressed as:

$$\rho(p,t) = \rho_0\left(1 + \frac{0.6\times10^{-9}\,p}{1+1.7\times10^{-9}\,p} - 0.00065(t-t_0)\right) \quad (19)$$

$$\eta(p,t) = \eta_0 \exp\left\{A_1\left[-1+(1+A_2 p)^z\left(\frac{t-138}{t_0-138}\right)^{-s_0}\right]\right\} \quad (20)$$

Where $A_1 = \ln\eta_0 + 9.67$, $A_2 = 5.1\times10^{-9}$, $z = \alpha/(A_1A_2)$, $s_0 = \beta/(A_1(t_0-138))$.

ii. *The film thickness is given as*

$$h = h_0 + \frac{x^2}{2R} - \frac{4}{\pi E}\int_{x_a}^{x_b} p(x)\ln|x-s|ds \quad (21)$$

Where$h_0$is film thickness constant depend on the applied load.

iii. *The balanced load equation*

The hydrodynamic pressure of the contact region must be in equilibrium with the input load, which calculated by the numerical method in section 2.Thus the pressure equilibrium is expressed by the following equation:

$$w = \int_{x_a}^{x_b} p(x)dx \quad (22)$$

The three-dimensional temperature distribution of oil film was calculated by the energy equation as follows:

$$\overbrace{\rho\cdot c_p(u\frac{\partial t}{\partial x})}^{\text{Convection}} - \overbrace{\lambda\frac{\partial^2 t}{\partial z^2}}^{\text{Heat Conduction}} + \overbrace{\frac{t}{\rho}\frac{\partial\rho}{\partial t}u(\frac{\partial p}{\partial x})}^{\text{Compression / Expation}} = \overbrace{\eta\left(\frac{\partial u}{\partial z}\right)^2}^{\text{FluidFriction}} \quad (23)$$

The boundary condition for Eq.23 is the thermal interface equation:

$$\begin{cases} t(x,0) = \dfrac{\lambda}{\sqrt{\pi\rho_1 c_1 u_1 \lambda_1}}\displaystyle\int_{-\infty}^{x}\frac{\partial t}{\partial z}\Big|_{z=0}\frac{ds}{\sqrt{x-s}} + t_a \\ t(x,h) = \dfrac{\lambda}{\sqrt{\pi\rho_2 c_2 u_2 \lambda_2}}\displaystyle\int_{-\infty}^{x}\frac{\partial t}{\partial z}\Big|_{z=h}\frac{ds}{\sqrt{x-s}} + t_b \end{cases}$$

Where t_a and t_b are the bulk interface temperature of the pinion and gear.

The equation governing the shear stress in the lubricant film is a momentum equation which for the Newtonian fluid is as follow:

$$\frac{\partial p}{\partial x} = \frac{\partial}{\partial z}\left(\eta\frac{\partial u}{\partial z}\right) \quad (24)$$

iv. *Numerical method*

All equations and boundary conditions mentioned above about thermal were written into dimensionless forms to facilitate the numerical calculation. There are pressure loop and temperature loop in the entire calculation process. In the pressure loop, assuming the temperature of all the nodes is the ambient temperature (360K). In the contact coordinate in the rolling direction (x direction), the whole contact region (from inlet position to outlet position) was divided into 81 non-equidistant nodes; the interval is large in the inlet region and small in the secondary pressure peak region. The distribution of pressure and the film thickness can be calculated by the Newton-Raphson method depending on the Equ.17-24.Divided the film gap (obtained in the pressure loop, z direction) into 21 equidistant nodes. The temperature of all the nodes can be calculated depend on the equ.20-21 and equ.24-25.Then repeat these two processes until the pressure error less than10^{-5} .The lubricant properties are shown in Table 2.

Table 2: Material properties of the lubricant and gears

Symbol,unit	Value
Ambient viscosity of lubricant , η_0 ,Ns/m^2	0.08
Specific heat of lubricant, c, J/kgK	2000
Specific heats of solids,J/kgK	470
Thermal conductivity of lubricant, λ , W/mK	0.14
Thermal conductivities of solids a and b, λ_1 and λ_2 ,W/mK	46
Ambient density of lubricant, ρ , kg/m^3	870
Densities of solids a and b, ρ_1 and ρ_2 , kg/m	7850
Barus viscocity–pressure coefficient, α , m^2/N	2.19×10^{-8}
Reynolds viscosity–temperature coefficient, β ,K^{-1}	0.042

IV. Thermal EHL Results

a) The thermal EHL results of the contact point

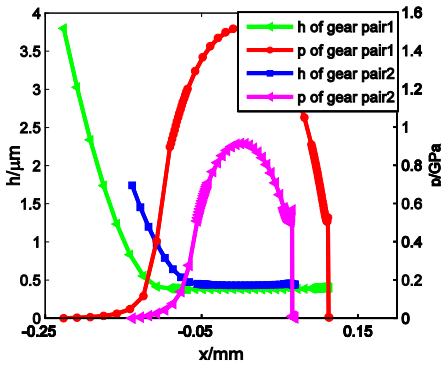

Fig. 20: The pressure and film thickness of oil film

Fig.20 shows the oil pressure and film thickness along the x direction of began meshing point of gear pair one and two. The load per unit of length of gear pair one is 2.73×10^5 N/m, and for gear pair two is 1.02×10^5 N/m shown in Fig.14. For the gear transimission system under heavy load, the film center pressure is higher; in this case, the maximum pressure is as high as 1.51GPa, the minimum film thickness is 0.42 μm. Because of the heavy load, the curve of oil pressure and oil thick has't the typical characteristic of thermal EHL. The secondary pressure peak close to the outlet and inconspicuous. The distribution of the pressure is similar to Hertzian pressure distribution. The maximum occurs the location x=0 and the heavier of the load, the higher of the maximum. The heavier, the wider the contact zone. Furthermore, it has little influence on the minimum oil thickness.

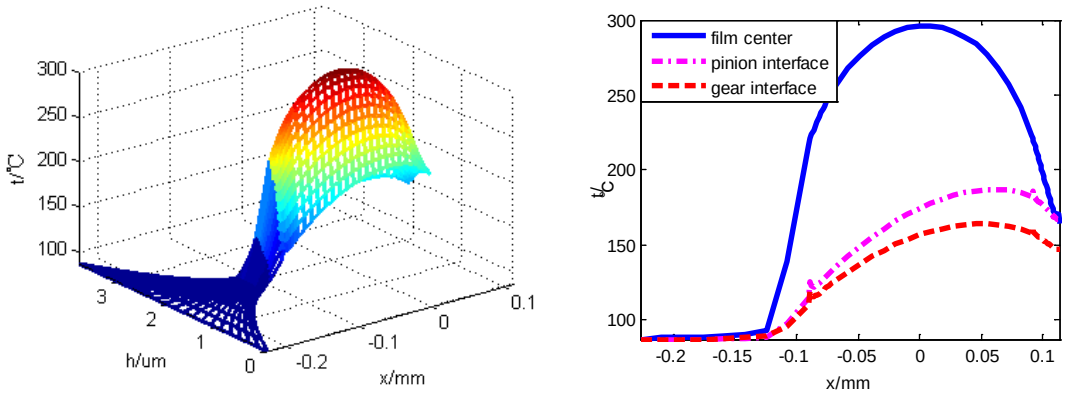

Fig. 21: Three-dimension film temperature and film center and interface temperature of gear pair1

The three-dimension and boundaries temperature distribution of the contact region are shown in Fig.21. The film center temperature is much higher than two boundaries; this is because the heat conducts from the film to all the teeth to maintain the bulk temperature. The distribution of film center temperature is similar to the film center pressure and peaked in the Hertzian maximum, but two boundaries are different from the film center; the temperature increase until close to the outlet and slightly decrease. The reason is in the rear part of the contact zone, the compression effect is no longer generate the heat, so the heat from the film center to the two boundaries via conduction effect and to the inner tooth through convection.

b) Comparison with the Blok's flash temperature

The contact and flash temperature is the main reason for the gear scuffing failure, Blok derived the flash temperature equation in 1937[12] as follow:

$$t_f = 0.7858\frac{fw|u_1-u_2|}{(\sqrt{\lambda_1\rho_1c_1u_1}+\sqrt{\lambda_2\rho_2c_2u_2})\sqrt{b_0}} \quad (25)$$

Where f=0.06 is coefficient of friction, w the load per unit of length, λ_i,ρ_i,c_i,u_i the heat conduction coefficient, density, specific heat, sliding speed of the pinion and gear,b_0 the half-width of Hertzian line contact.

In the thermal EHL results, the maximum temperature rise of two boundaries is its flash temperature. The flash temperature along the feature coordinate was calculated by the thermal EHL method and Blok equation as show in Fig.22. In the dedendum region of the pinion (close to approach point), the thermal EHL flash temperature is higher than the Blok result, and in the addendum region of the pinion(close to recess point), the Blok temperature is lower than thermal EHL flash temperature. In theory, the temperature-pressure-density and temperature-pressure-viscosity effect and the compression of oil film were considered in the thermal EHL theory. The Blok flash temperature equation is very concise and corresponding to the experiment to some extent. However, it loses sight of the influence of the bulk temperature, so it is not a good agreement of the experiment under the heavy load. Thus the thermal EHL theory is even close to the actual condition. The safety factor defined as follow [10]:

$$S = \frac{t_s - t_{oil}}{t_{c\max} - t_{oil}} \tag{26}$$

Where t_s is the scuffing temperature, t_{oil} the ambient temperature, t_{cmax} the maximum contact temperature.

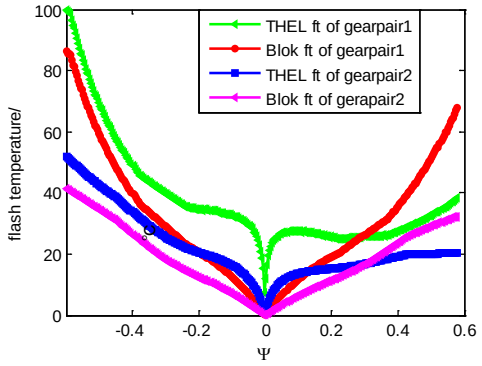

Fig. 22: The TEHL flash temperature and Blok flash temperature of the helical gear in the feature coordinate

c) *The minimum thickness method from thermal EHL and Dowson equation*

When gear teeth are separated completely by a full fluid film of lubricant, there is no contact between the asperities of tooth surfaces, and usually, there is no scuffing and wear. For the heavy load helical gear, the thickness of oil film is very small, and incidental asperity contact takes place. As the minimum film thickness decreases, the number of contacts increases, abrasive wear, adhesive wear, and scuffing became possible. So the minimum thickness of lubricant film is a property of scuffing load capacity, especially for the gear pair under heavy load. The minimum thickness equation was given by Dowson and Higginson [22] as the Equ.27. The safe factor can be measured by the thickness ratio. When the thickness ratio $\chi \subset [1,4]$,it is considered as mixed friction. When the thickness ratio is less than 1, the scuffing failure probably takes place to a great extent.

$$h_{\min} = \frac{2.65\alpha^{0.54}(\eta_0 u_m)^{0.7} R^{0.43}}{E^{0.03} w^{0.13}} \tag{27}$$

$$\chi = h_{\min} / \sqrt{R_{a1}^2 + R_{a2}^2} \tag{28}$$

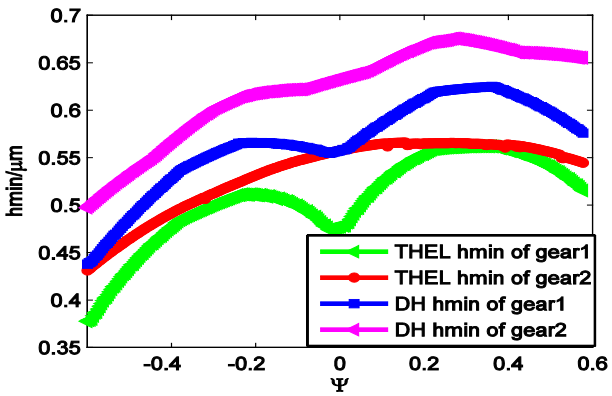

Fig. 23: The minimum thickness of the film in the feature coordinate system

The minimum film thickness solved by thermal EHL and Dowson equation is shows as Fig.23. The minimum thickness curves are similar along the feature coordinate of gear pair one and two. The minimum film thick is lowest in the dedendum of the pinion, so the dedendum of the pinion is dangerous. The results are consistent with the maximum flash temperature method. The value from thermal EHL is lower than that from the Dowson equation. The Dowson equation didn't consider the influence of temperature on film thickness.

In contrast to the fatigue damage, a single momentary overload may initiate scuffing failure, so the scuffing capacity is crucial for the heavy load and high-speed helical gear system. The minimum film thickness and maximum contact temperature, as well as the flash temperature obtained by the thermal EHL theory, are applied to check the scuffing strength. The scuffing capacity can be checked by the flash temperature or minimum thickness method.

V. Conclusions

In this paper, a model of non-uniform along the contact line of helical gear teeth, obtained from the meshing stiffness, transmission error, and balanced load equation, has been proposed. The feature coordinate system was established to simply preliminary design and strength rating process. The thermal effect of helical gear lubrication will affect the scuffing load capacity. The thermal EHL method is applied to check the scuffing load capacity.

The following conclusions can be drawn:

1. The length of contact lines depends on the face width and basic helix angle. And the length is oline is not paralleled with the axial line. The fluctuation is evident when the total contact ratio less than 2.The distribution of transmission error is similar to the sum length. The distribution of load per unit of length is dependent on the meshing stiffness and transmission, it is similar to the meshing stiffness along the contact line and similar to the transmission error along the *B*axis. The modification of gears can greatly improve the distribution of contact stress. The maximum contact stress is concentrated in the center of the tooth surface to avoid the contact between the tooth surface. The contact stress inclines to one end, and the maximum stress is also increasing under with misalignment.
2. The feature coordinate system established in this paper can cover bother the tooth profile and axial information. It can satisfy the need for preliminary design and strength check of helical gears. The weakest strength region is the dedendum of the pinion. A load of the dedendum region in the feature coordinate system is as same as the three-dimension coordinates system.
3. The thermal EHL theory can provide more information to check the scuffing load capacity. The highest contact temperature and minimum film thickness method were applied to evaluate the scuffing load capacity. The pressure distribution under heavy load is similar to the Hertzian pressure distribution, and the secondary presser peak close the outlet and inconspicuous. The temperature of the film center is much higher than two boundaries. The film center temperature distribution is similar to the pressure distribution. The two boundaries temperature increase until close to the outlet and slightly decrease. The thermal EHL flash temperature is corresponding to the Blok flash temperature but higher in the dedendum region and lower in the addendum region of the pinion. The minimum thickness film is smaller than the Dowson equation. So the scuffing load capacity that solved by thermal EHL is more practical than the traditional method.

References Références Referencias

1. ISO Standard 6336-2:1996, Calculation of Load Capacity of Spur and Helical Gears – Part 2: Calculation of Surface Durability (Pitting), International Organization for Standardization, Geneva, Switzerland, 1996.
2. ISO Standard 6336-3:1996, Calculation of Load Capacity of Spur and Helical Gears – Part 3: Calculation of Tooth Bending Strength, International Organization for Standardization, Geneva, Switzerland, 1996.
3. Zaigang Chen, Yimin Shao. Mesh stiffness calculation of a spur gear pair with tooth profile modification and tooth root crack. Mechanism and Machine Theory, 62(2013)63-74.
4. A. Fernandez del Rincon, F. Viadero, M. Iglesias, et al. A model for the study of meshing stiffness in spur gear transmissions. Mechanism and Machine Theory, 61(2013)30-58.
5. Y. Zhang, Z. Fang. Analysis of tooth contact and load distribution of helical gears with crossed axes. Mechanism and Machine Theory. 34(1999)41-57.
6. I Yesilyurt, FS Gu, Andrew D. Ball. Gear tooth stiffness reduction measurement using modal analysis and its use in wear fault severity assessment of spur gears. NDT&E International. 36(2003)357-372.
7. J.I.Pedrero, M.Pleguezuelos, M.Artés, J.A.Antona, Load distribution model along the line of contact for involute external gears, Mechanism and Machine Theory 45 (2010)780-794.
8. J.I.Pedrero, M.Pleguezuelos, M.Muñoz. Critical stress and load conditions for bending calculations of spur and helical gear, International Journal of Fatigue 48 (2013)28-38.

9. J.I. Pedrero, M.Pleguezuelos, M.Muñoz. Critical stress and load conditions for pitting calculations of spur and helical gear, Mechanism and Machine Theory 46(2011)425-437.
10. ISO Standard 13989-1:2000, Calculation of scuffing load capacity of cylindrical, bevel and hypoid gears-Part 1: Flash temperature method. British Standards Institution, London, 2000.The United Kingdom.
11. ISO Standard 13989-2:2000, Calculation of scuffing load capacity of cylindrical, bevel and hypoid gears-Part 1: Integral temperature method. British Standards Institution, London, 2000.The United Kingdom.
12. H.Blok. Theoretical study of temperature rise at surfaces of actual contact under oiliness lubricating conditions, in Proceedings of the General Discussion on Lubrication and Lubricants[J]. Imech E, 2(1937)222–235.
13. Wang KL, Cheng HS. Anumerical solution to the dynamic load, film thickness and surface temperatures in spur gears, part I analysis. Journal of Mechanical Design. 103(1981)177–187.
14. Wang KL, Cheng HS. A Numerical solution to the dynamic load, film thickness and surface temperatures in spur gears, part II results. Journal of Mechanical Design.103 (1981)188–194.
15. Li-Ming Chu, Hsiang-Chen Hsu, Jaw-Ren Lin, dtal. Inverse approach for calculating temperature in EHL of line contacts. Tribology International. 42 (2009)1154-1162.
16. T.Almqvist, R. Larsson. The Navier–Stokes approach for thermal EHL line contact solutions. Tribology International. 35(2002)163-170.
17. P. Anuradha, Punit Kumar. Effect of lubricant selection on EHL performance of involute spur gears. Tribology International. 50 (2012)82-90.
18. Lars Bobach, Ronny Beilicke, Dirk Bartel, et al. Thermal elastohydrodynamic simulation of involute spur gears incorporating mixed friction. Tribology International, 48 (2012)191-206.
19. P.W. Wang, H.Q. Li, J.W. Tong, et al. Transient thermo elastohydrodynamic lubrication analysis, Tribology International, 37(2004)773-782.
20. Ping Yang, Peiran Yang. Analysis on the thermal elastohydrodynamic lubrication of tapered rollers in opposite orientation. Tribology International, 40(2007)1627-1637.
21. Roelands CJA. Correlation aspects of Viscosity-temperature-pressure Relationship of Lubrication oils. Delft Univeristy of Technology, Netherlands, 1966.
22. Dowson D, Higginson GR. Elastohydrodynamic Lubrication. Oxford: Pergamon Press, 1977.